



HAL
open science

Stepwise Functionalization of a Pillar[5]arene-Containing [2]Rotaxane with Pentafluorophenyl Ester Stoppers

Nihed Becharguia, Emeric Wasielewski, Rym Abidi, Iwona Nierengarten,
Jean-françois Nierengarten

► To cite this version:

Nihed Becharguia, Emeric Wasielewski, Rym Abidi, Iwona Nierengarten, Jean-françois Nierengarten. Stepwise Functionalization of a Pillar[5]arene-Containing [2]Rotaxane with Pentafluorophenyl Ester Stoppers. *Chemistry - A European Journal*, 2023, 30, 10.1002/chem.202303501 . hal-04518699

HAL Id: hal-04518699

<https://hal.science/hal-04518699>

Submitted on 24 Mar 2024

HAL is a multi-disciplinary open access archive for the deposit and dissemination of scientific research documents, whether they are published or not. The documents may come from teaching and research institutions in France or abroad, or from public or private research centers.

L'archive ouverte pluridisciplinaire **HAL**, est destinée au dépôt et à la diffusion de documents scientifiques de niveau recherche, publiés ou non, émanant des établissements d'enseignement et de recherche français ou étrangers, des laboratoires publics ou privés.

Hot Paper

Special
Collection

Stepwise Functionalization of a Pillar[5]arene-Containing [2]Rotaxane with Pentafluorophenyl Ester Stoppers

Nihed Becharguia,^[a, b] Emeric Wasielewski,^[c] Rym Abidi,^[b] Iwona Nierengarten,^{*[a]} and Jean-François Nierengarten^{*[a]}*Dedicated to Prof. Maurizio Prato on the occasion of his 70th birthday.*

Detailed investigations into the stepwise bis-functionalization of a pillar[5]arene-containing rotaxane building block have been carried out. Upon a first stopper exchange, the pillar[5]arene moiety of the mono-acylated product is preferentially located close to its reactive pentafluorophenyl ester stopper, thus limiting the accessibility to the reactive carbonyl group by the nucleophilic reagents. Selective mono-functionalization is thus very efficient. Introduction of a second stopper is then possible to generate dissymmetrical rotaxanes with different amide

stoppers. Moreover, when dethreading is possible upon the second acylation, the pillar[5]arene plays the role of a protecting group allowing the synthesis of dissymmetrical axles that are particularly difficult to prepare under statistical conditions. Finally, detailed conformation analysis of the rotaxanes revealed that the position of the pillar[5]arene moiety on its axle subunit is mainly governed by polar interactions in nonpolar organic solvents, whereas solvophobic effects play a major role in polar solvents.

Introduction

The chemistry of mechanically interlocked molecules (MIMs) has been mainly focused on the development of new synthetic strategies for their preparation.^[1,2] As soon as efficient methodologies were developed, the pioneering work of Sauvage and Stoddart revealed that MIMs are perfectly suited compounds for the preparation of molecular machines.^[3,4] MIMs are indeed able to adopt very different conformations that can be interconverted in a controlled manner by applying appropriate chem-

ical, electrical or optical stimuli.^[5] On the other hand, the intertwined structure of MIMs provides also a noncovalent shielding protective effect decreasing the reactivity of some of their subunits.^[6-9] This effect has been beautifully exploited by Anderson and co-workers to enhance the photostability of azo and cyanine dyes encapsulated in macrocyclic components of rotaxanes.^[7-8] Similarly, sensitive molecular wires such as cumulenes or oligoynes have been also stabilized by a surrounding macrocycle in rotaxane architectures.^[9] In contrast, the chemical reactivity of MIMs has been largely overlooked.^[6] Moreover, only a few examples of post-synthetic modifications in which the mechanical bonds alter the chemical reactivity of one component in interlocked structures have been investigated so far.^[10] As part of this research, our group became recently interested in the preparation of versatile pillar[5]arene-containing rotaxane building blocks equipped with activated stoppers allowing the synthesis of a large variety of derivatives by stopper exchange reactions.^[11-13] As these chemical transformations occurred by either an addition/elimination mechanism or a concerted nucleophilic substitution, no intermediate allows for the disassembly of the interlocked molecular ensemble and the rotaxane structure is fully preserved during the stopper exchange reactions. In this paper, we now report on a stepwise functionalization of a symmetrical pillar[5]arene-based building block. As the first stopper exchange reaction is fast and the second always significantly slower, mono-functionalization of the rotaxane building block can be selectively achieved. Therefore, the stepwise bis-functionalization of the rotaxane starting material is easily carried out to generate unsymmetrical rotaxanes with two different stoppers in excellent yields. Moreover, we have also shown that the pillar[5]arene moiety can act as a protecting group allowing the efficient synthesis of unsymmetrically substituted compounds

[a] N. Becharguia, Dr. I. Nierengarten, Dr. J.-F. Nierengarten
Laboratoire de Chimie des Matériaux Moléculaires
Université de Strasbourg et CNRS (UMR 7042 LIMA)
Ecole Européenne de Chimie, Polymères et Matériaux
25 rue Becquerel, 67087 Strasbourg Cedex 2 (France)
E-mail: iosinska@unistra.fr
nierengarten@unistra.fr
Homepage: <http://nierengartengroup.com>

[b] N. Becharguia, Prof. R. Abidi
Laboratoire d'Applications de la Chimie aux Ressources et
Substances Naturelles et l'Environnement
Faculté des Sciences de Bizerte, Université de Carthage
7021 Zarzouna Bizerte (Tunisia)

[c] Dr. E. Wasielewski
Plateforme RMN Cronembourg
Université de Strasbourg et CNRS (UMR 7042 LIMA)
Ecole Européenne de Chimie, Polymères et Matériaux
25 rue Becquerel, 67087 Strasbourg Cedex 2 (France)

Supporting information for this article is available on the WWW under <https://doi.org/10.1002/chem.202303501>

This article is part of a joint Special Collection in honor of Maurizio Prato.

© 2023 The Authors. Chemistry - A European Journal published by Wiley-VCH GmbH. This is an open access article under the terms of the Creative Commons Attribution Non-Commercial NoDerivs License, which permits use and distribution in any medium, provided the original work is properly cited, the use is non-commercial and no modifications or adaptations are made.

particularly difficult to prepare from a bifunctional starting material lacking the macrocyclic moiety. Finally, detailed NMR studies of the unsymmetrical [2]rotaxanes have been also carried out to fully understand the influence of weak polar interactions on their conformational preferences.

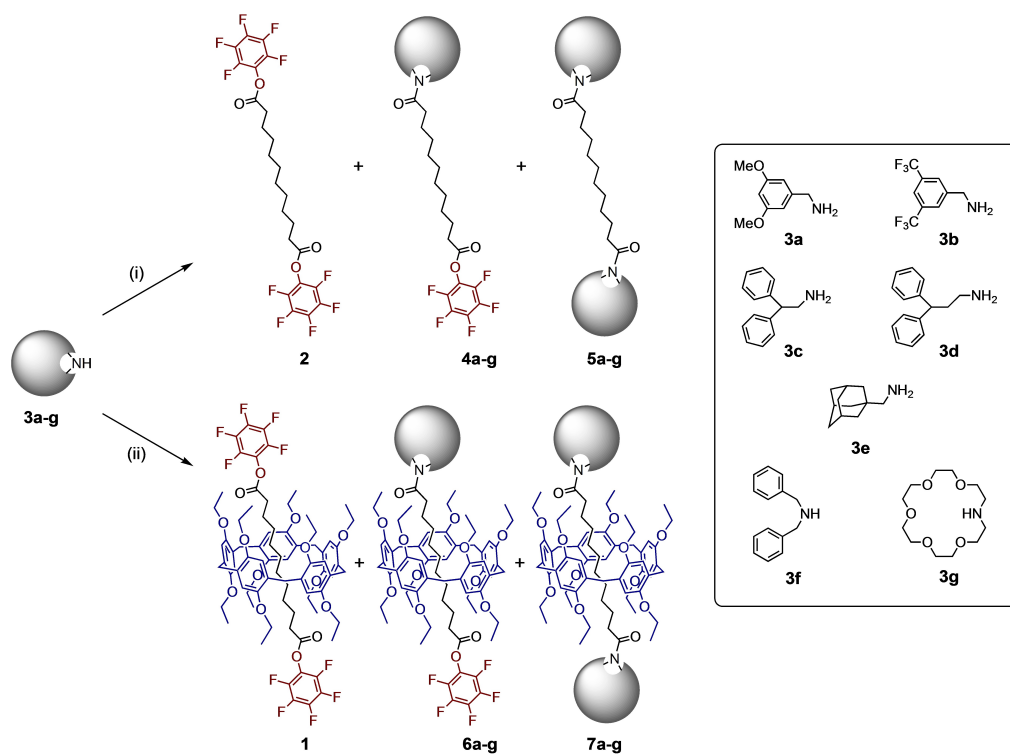
Results and Discussion

Stepwise stopper exchange

Rotaxane building block **1** was prepared as reported in the literature (Scheme 1).^[12] We have shown that reaction of **1** with nucleophiles such as amines gave access to a wide range of symmetrical rotaxanes with two identical amide stoppers.^[12] Interestingly, it was noticed that the first addition-elimination was very fast but the second one significantly slower. This observation suggested that steric hindrance resulting from the presence of the macrocycle close to the pentafluorophenyl ester stopper in the intermediate mono-acylated product may limit the accessibility of the amine nucleophile for the second stopper exchange. In order to evaluate the effect of the pillar[5]arene moiety on the reactivity of the pentafluorophenyl ester subunits in rotaxane **1**, both **1** and model compound **2** were treated with one equivalent of various primary amine reagents (**3 a–e**). All the reactions were performed in THF at 0 °C (Scheme 1). After 3 h, the resulting mixtures were filtered over a short plug of silica gel and the crude materials directly analyzed

by ¹H NMR spectroscopy to evaluate the outcome of the reactions.

Secondary amine reagents **3 f** and **3 g** were also used. In these particular cases, completion of the reactions with axle **2** required 12 h at 0 °C. At this temperature, no reaction was observed between **3 f** and **3 g** and rotaxane **1** thus already highlighting a significant influence of the pillar[5]arene moiety on the reactivity of its pentafluorophenyl ester moieties. In the case of **1**, complete consumption of the secondary amine reagents was only observed after several days at room temperature. Again, the outcome of these reactions was directly analyzed by recording ¹H NMR spectra of the resulting crude materials. In all the cases, the relative proportion of starting material, mono- and bis-acylated products was derived from the integration of the ¹H NMR spectra recorded for the crude materials. The results are summarized in Table 1. In the case of axle **2**, the two reactive pentafluorophenyl ester subunits are independent and equivalent. As expected, the treatment of **2** with one equivalent of amine nucleophiles **3 a–g** always yielded unreacted **2**, **4 a–g** and **5 a–g** in a statistical 1:2:1 relative ratio. Interestingly, this is not the case anymore when starting from rotaxane **1**. Effectively, formation of the mono-acylated product was always largely favored thus revealing that the second acylation of **6 a–g** leading to **7 a–g** is much slower when compared to the first acylation of starting material **1**. This kinetic selectivity is ascribed to steric effects resulting from the presence of the pillar[5]arene moiety that must be likely attracted by the electro-deficient pentafluorophenyl stopper in **6 a–g** and thus limiting the accessibility of its reactive penta-



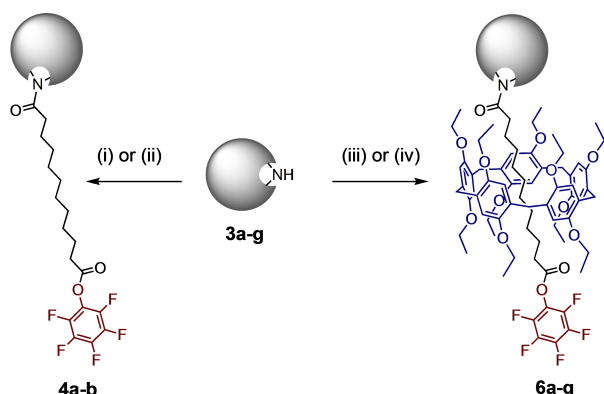
Scheme 1. Treatment of building blocks **1** and **2** with amine reagents **3 a–g** (1 equiv.). The proportions of starting material, mono-acylated and bis-acylated products were determined based on analysis of the ¹H NMR spectra recorded for the crude products (Table 1). i) **2** (2 equiv.), THF, 0 °C; ii) **1** (1 equiv.), THF, 0 °C for **3 a–e** and RT for **3 f** and **g**.

Table 1. Relative proportion of starting material, mono- and bis-acylated products derived from integration of the ^1H NMR spectra recorded for the crude materials resulting from the reaction of **1** and **2** with 1 equiv. of amine reagents **3a–g** in THF at 0°C for 3 h (**3a–e**) or at RT for 3 days (**3f** and **g**).

Amine	2/4a–g/5a–g	1/6a–g/7a–g
3a	24/52/24	3/94/3
3b	25/50/25	7/87/6
3c	23/51.3/25.7	3/94/3
3d	28/48/24	10/81/9
3e	25/50/25	13/74/13
3f	25/50/25	19/76/5
3g	25/50/25	5/90/5

fluorophenyl ester group. This view was fully supported by the detailed analysis of the ^1H NMR spectra of **6a–g** (see below). It is also worth noting that the temperature plays an important role in the preferential formation of mono-amides **6a–g**. Effectively, the selectivity was significantly decreased when the reaction was performed at room temperature rather than at 0°C . This observation also fully supports the kinetic origin for the selective formation of mono-amides from symmetrical building block **1**.

The reaction conditions were then optimized for the preparative synthesis of mono-acylated products from **1** and amine reagents **3a** and **3b** (Scheme 2). Treatment of amines **3a** and **b** with a one equiv. of **1** in THF at 0°C provided mainly the desired mono-amide products but small amounts of diacylated byproducts were also formed under these conditions. Compounds **6a** and **6b** were then isolated in a pure form in 94 and 87% yields, respectively. By using an excess of **1** (2 equiv.), only residual traces of diacylated byproducts were observed and the mono-acylated products were almost exclusively obtained. The excess of starting rotaxane **1** and products **6a** and **b** were then easily separated by column chromatography on silica gel owing to a large difference in polarity. Compounds **6a** and **6b** were



Scheme 2. Preparation of mono-acylated products from building blocks **1** and **2**. i) **2** (2 equiv.), THF, 0°C (**4a**: 66%; **4b**: 61%); ii) **2** (3 equiv.), THF, 0°C (**4a**: 88%; **4b**: 75%); iii) **1** (1 equiv.), THF, 0°C (**6a**: 94%; **6b**: 87%); iv) **1** (2 equiv.) THF, 0°C for **3a–e** and RT for **3f–g** (**6a**: 98%; **6b**: 97%; **6c**: 91%; **6d**: 94%; **6e**: 98%; **6f**: 98%; **6g**: 91%).

isolated in 98 and 97% yields, respectively. Importantly, treatment of **3a** and **b** (1 equiv.) with model compound **2** (2 equiv.) under the same conditions provided the corresponding mono-amide products (**4a** and **b**) with significant amounts of diacylated byproducts **5a** and **b**. Under these conditions, compounds **4a** and **4b** were isolated in 66 and 61% yields, respectively. By further increasing the excess of **2** (3 equiv.), the yields in **4a** and **4b** were improved to 88 and 75%, respectively. However, significant amount of bis-acylated were still obtained under these conditions.

The conditions optimized for the preparation of **6a** and **b** were then used for the synthesis of compounds **6c–g**. For primary amines **3c–e**, treatment with an excess of **1** (2 equiv.) in THF at 0°C provided mono-amide rotaxanes **6c–e** in excellent yields. With the secondary amine reagents **3f** and **g**, the reactions with **1** were carried out at room temperature. Compounds **6f** and **6g** were thus obtained in very good yields.

Mono-amide rotaxanes **6a–g** were fully characterized by NMR and IR spectroscopies and mass spectrometry. Crystals suitable for X-ray crystal structure analysis were obtained for both **6a** and **6b**. The structures are shown in Figure 1. Owing to their D_5 -symmetry imposed by their pillar[5]arene subunit, compounds **6a** and **6b** are chiral. Close inspection of the crystal lattice revealed that both **6a** and **6b** crystallized as racemates. As shown in Figure 1, π -stacked pairs of enantiomers with opposite chirality are effectively observed in both cases. Further inspection of the supramolecular organization within the crystals of **6a** and **6b** revealed a very similar packing. Indeed, both compounds gave crystals belonging to the same monoclinic lattice for space group 14, namely $P2_1/c$ for **6a** and $P2_1/n$ for **6b**. These space groups refer actually to the same lattice but they differ in the choice of the axes used to define the unit cell. Both **6a** and **6b** adopt a similar conformation in the solid state. Moreover, similar intermolecular interactions are observed between neighboring molecules in the two crystal lattices. In

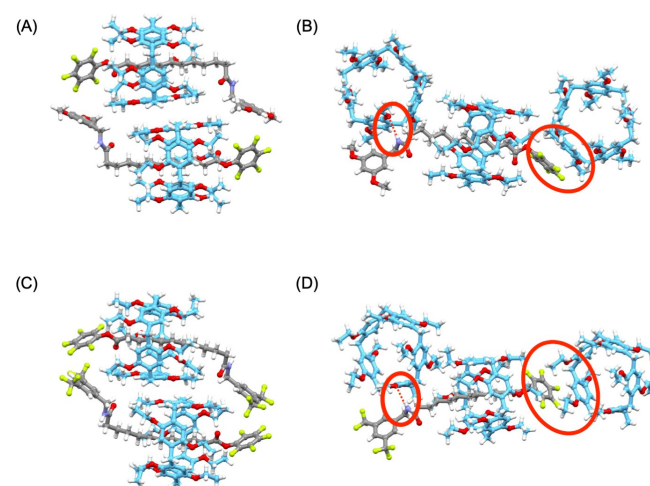


Figure 1. Pairs of enantiomers observed in the X-ray crystal structures of A) **6a** and C) **6b**. Views highlighting remarkable intermolecular interactions within the crystal lattice of B) **6a** and D) **6b**; $\text{NH}\cdots\text{O}$ distances: 2.259 Å for **6a** and 2.365 Å for **6b** (H: white, F: light green, O: red, N: blue, C: grey for the axle and pale blue for the pillar[5]arene moiety).

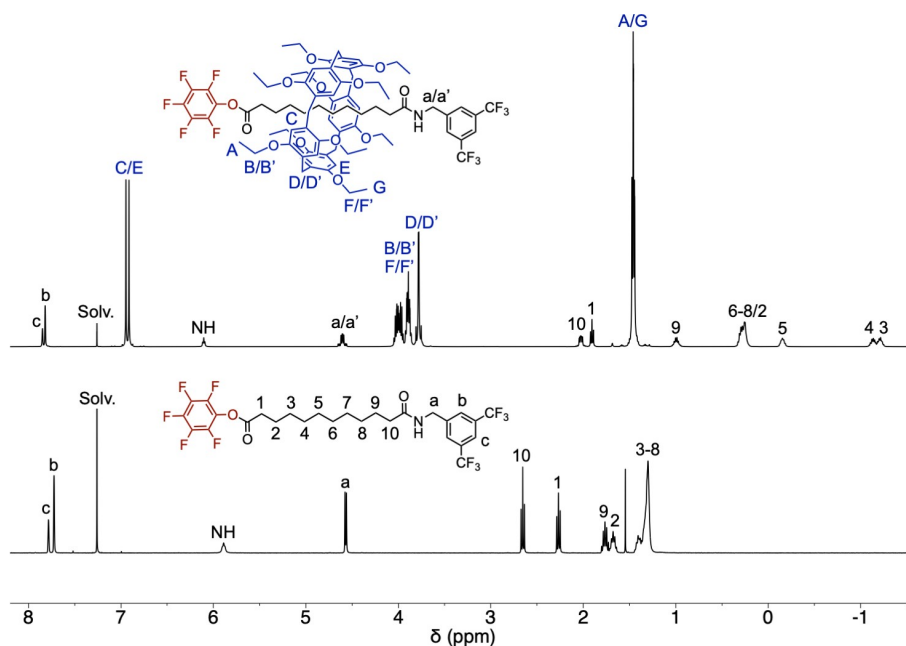


Figure 2. ^1H NMR spectra (500 MHz) recorded for **4b** and **6b** in CDCl_3 at 25°C .

both cases, the electron-deficient pentafluorophenol aromatic ring is interacting with the electron-rich hydroquinone subunit of a neighboring pillar[5]arene. In addition, the amide NH group of the axle of one rotaxane is interacting with the O atom of a pillar[5]arene moiety belonging to another neighboring rotaxane molecule. The establishment of this particular interaction is forcing the $-(\text{CH}_2)_{10}-$ chain of the axle moiety to adopt a tilted conformation. As a result, the pillar[5]arene moiety of the rotaxanes is pushed far from its amide stopper. The peculiar position of the macrocyclic moiety close to the pentafluorophenyl ester subunits observed in the solid state is therefore not ascribed to an attractive interaction of the pillar[5]arene for its more electro-deficient stopper but is more likely related to packing forces allowing to maximize favorable intermolecular H-bonding and π - π -stacking interactions within the crystal lattice of **6a** or **6b**.

In solution, dynamic gliding motions of the pillar[5]arene subunit along the $-(\text{CH}_2)_{10}-$ chain of the axle moiety of rotaxanes **6a–g** are expected. However, the observed kinetic effects allowing the preferential formation of mono-amides **6a–g** from **1** suggest that the pillar[5]arene is somehow attracted by its pentafluorophenyl ester stopper in **6a–g**. In order to support this hypothesis, the chemical shift observed in the ^1H NMR spectra for the methylene moieties of the $-(\text{CH}_2)_{10}-$ chain of rotaxanes **6a–g** were carefully analyzed. As a typical example, the ^1H NMR spectra recorded at 25°C in CDCl_3 for rotaxane **6b** and the corresponding axle **4b** are shown in Figure 2. When compared to axle **4a**, a dramatic shielding is observed for all the signals arising from the $-(\text{CH}_2)_{10}-$ chain for rotaxane **6b**. This is due to the ring current effect of the pillar[5]arene aromatic moieties on the CH_2 groups of the axle in **6b**. Clearly, all the methylene groups are affected thus showing that there is no preferential conformation. In other

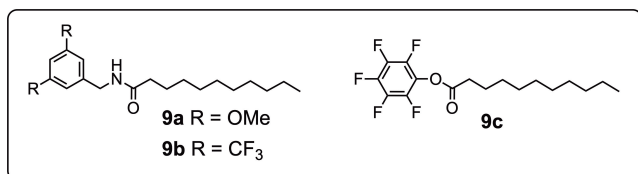
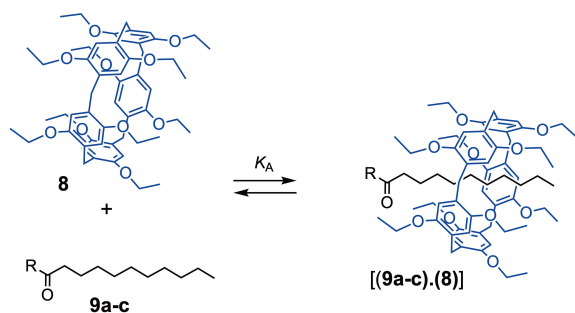
words, dynamic gliding motions of the pillar[5]arene subunit along the $-(\text{CH}_2)_{10}-$ chain must be very fast on the NMR timescale. However, the shielding effect is more important for H(2), H(3), H(4) and H(5) thus suggesting a higher probability of presence of the pillar[5]arene subunit over these specific positions. Therefore, the electron-rich macrocycle must be on average closer to the most electro-deficient stopper. Similar effects were also evidenced for **6a** and **6c–g**. (Table 2).

In all the cases, analysis of the chemical shifts observed for the methylene moieties of the $-(\text{CH}_2)_{10}-$ chain in the ^1H NMR of the dissymmetrical rotaxanes were fully consistent with a preferential presence of the macrocycle close to the pentafluorophenyl ester stopper. Favorable donor–acceptor electronic effects may therefore slightly lower the energy of this particular position explaining why it is more populated. As a result, the accessibility of the reactive carbonyl group in **6a–g** by nucleophilic reagents must be more difficult thus explaining well the efficient preparation of mono-amide rotaxanes from building block **1**. Interestingly, detailed analysis of the chemical shifts of the methylene groups of **6a–g** as a function of the amide stopper revealed also some interesting trends. The probability of presence of the macrocycle close to the pentafluorophenyl stopper is increased when the amide stopper is electron-rich (**6a**) or rather bulky (**6c**) as suggested by a more important shielding for the signals ascribed to H(2–5) and a less important one for those corresponding to the resonances of H(6–9). This view is fully consistent with the different relative proportions of starting material, mono- and bis-acylated products obtained in the initial reactions of **1** with primary amines **3a–e** (Scheme 1, Table 1), the preferential formation of mono-amide rotaxanes being effectively more favorable with amine reagents **3a** and **3c** when compared to the other ones.

Table 2. Chemical shifts (δ in ppm) of the methylene units of the $-(CH_2)_{10}-$ chain in the 1H NMR spectra recorded at 25 °C in $CDCl_3$ for dissymmetrical rotaxanes **6a–g** (for the numbering, see Figure 2).

Compound	H(1)	H(2)	H(3)	H(4)	H(5)	H(6)	H(7)	H(8)	H(9)	H(10)
6a	1.86	−0.05	−1.83	−1.69	−0.38	0.34	0.63	0.86	1.45	2.11
6b	2.02	0.31	−1.18	−1.11	−0.17	0.20	0.20	0.20	0.94	1.87
6c	1.71	−0.31	−2.25	−2.07	−0.56	0.35	0.83	1.08	1.50	2.04
6d	1.86	−0.06	−1.85	−1.70	−0.36	0.37	0.67	0.85	1.36	1.98
6e	1.81	−0.22	−2.13	−1.93	−0.41	0.49	0.97	1.24	1.68	2.26
6f	1.77	−0.27	−2.25	−2.04	−0.44	0.52	1.08	1.35	1.86	2.56
6g	1.69	−0.37	−2.35	−2.11	−0.48	0.50	1.04	1.29	1.69	2.42

To fully understand the influence of the different stoppers on the conformational equilibria observed for rotaxanes **6a–g**, the formation of host–guest complexes between pillar[5]arene **8** and model compounds **9a–c** was investigated (Figure 3). The ability of **9a–c** to form inclusion complexes with pillar[5]arene **8** was investigated by 1H NMR binding studies in $CDCl_3$ at 298 K. The association constants (K_A) for the 1:1 complexes were

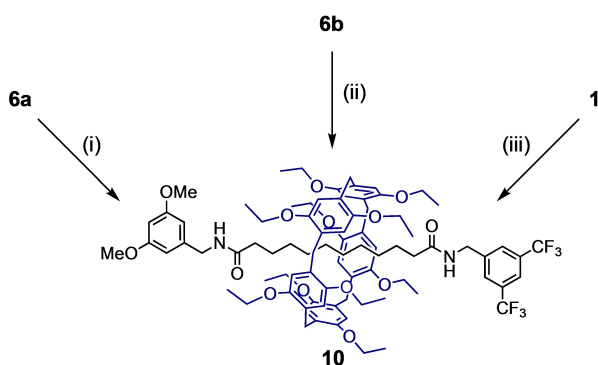
**Figure 3.** The formation of host–guest complexes from model compounds **9a–c** and pillar[5]arene **8**; the $\log K_A$ values derived from 1H NMR binding studies in $CDCl_3$ at 298 K are 0.38 (2) for **9a**, 0.82 (1) for **9b** and 1.08 (2) for **9c**.

estimated on the basis of the complexation-induced changes in chemical shift by using curve fitting analysis. The $\log K_A$ values thus obtained are 0.38(2) for **9a**, 0.82(1) for **9b** and 1.08(2) for **9c**. The formation of the host–guest complex is significantly more favorable for guest **9c**. These observations are fully consistent with the observed conformational preferences for rotaxanes **6a** and **6b**, and explains well why the peripheral position of the pillar[5]arene close to the pentafluorophenyl ester stopper is favored.

Having now in hand an efficient procedure to easily produce dissymmetrical rotaxane building blocks from **1**, we decided to further investigate their possible functionalization to produce rotaxanes with two different amide stoppers.^[14] As shown in Scheme 3, treatment of **6a** with amine **3b** in THF at room temperature gave rotaxane **10** with two different amide stoppers. The preparation of **10** was also performed by reversing the order of the successive stopper exchange reactions. Specifically, reaction of **6b** with amine **3a** afforded **10** in a good yield.

Compound **10** was also directly prepared from **1** by a one-pot approach. In this particular case, the order of addition of the different amine reagents was important. It was decided to use amine **3a** first as this reagent was more selective for the preparation of a mono-amide intermediate (Table 1). Rotaxane **1** was thus first treated with amine **3a** (1 equiv.) in THF at 0 °C. Upon 3 h, **3a** was totally consumed and the second amine reagent, namely **3b**, was added to the reaction mixture and the temperature increased to room temperature. Compound **10** was thus obtained in 89% yield.

Rotaxane **10** was characterized by a combination of different analytical tools. Crystals suitable for X-ray crystal analysis were obtained by slow diffusion of acetonitrile into a $CH_2Cl_2/MeOH$ solution of **10**. As shown in Figure 4, compound **10** co-crystallized with a methanol molecule that is interacting with the O atom of a carbonyl group of the axle moiety of the rotaxane through a H-bond. In addition to the classical intermolecular C–H $\cdots\pi$ interactions between the aromatic moieties of the pillar[5]arene subunit and the methylene groups of the axle located within its cavity,^[12] the occurrence of an intramolecular H-bond between one NH of the axle and an oxygen of the pillar[5]arene subunit is also observed. Interestingly, the dodecyl chain of **10** does not adopt a fully extended conformation but is folded. As already observed in the crystal

**Scheme 3.** Preparation of compound **10**. i) **3b**, THF, RT (93%); ii) **3a**, THF, RT (98%); iii) **3a**, THF, 0 °C, then **3b**, THF, RT (89%).

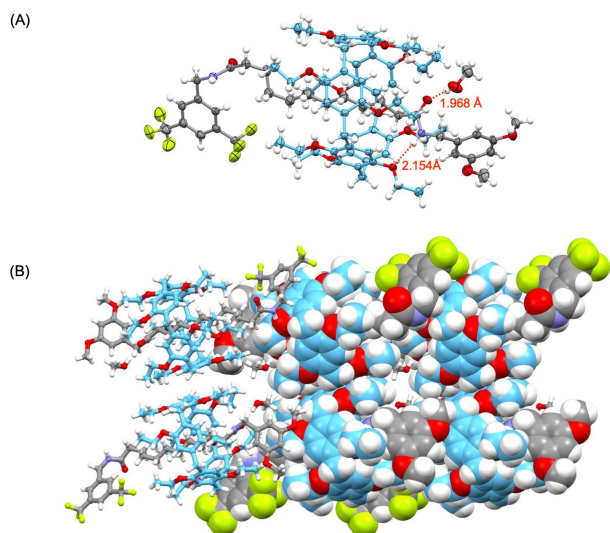


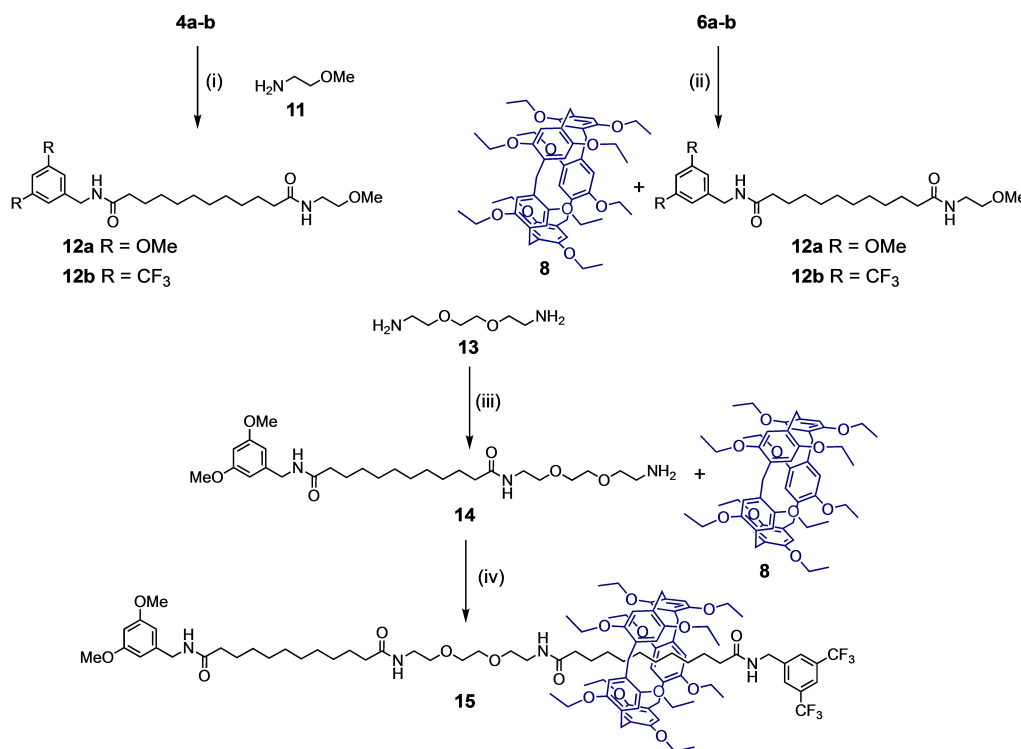
Figure 4. A) ORTEP plot of the structure of **10**-MeOH highlighting the intramolecular H-bond between the NH group of the axle and an O atom of the macrocycle as well as the H-bond between the axle and the co-crystallized solvent molecule (H: white, F: light green, O: red, N: blue, C: grey for the axle and pale blue for the pillar[5]arene moiety; the disorder of some CF₃ groups has been omitted for clarity; thermal ellipsoids are shown at 50% probability level). B) Stacking within the **10**-MeOH lattice highlighting the intermolecular π - π interactions between neighboring rotaxanes.

lattice of related rotaxanes,^[12,15] packing forces are likely responsible for the folding of the decyl chain in order to optimize favorable intermolecular contacts. This is fully sup-

ported by the observation of intermolecular π - π interactions between the electro-deficient bis(trifluoromethyl)phenyl rings with electron-rich hydroquinone moieties of neighboring pillar[5]arenes leading to the formation of infinite supramolecular chains in the crystal lattice (Figure 3B). Compound **10** is chiral and crystallized as a racemate. Indeed, the two enantiomers are organized in anti-parallel supramolecular chains interacting through π - π interactions between enantiomeric pillar[5]arene moieties.

The pillar[5]arene as a protecting group

The stopper exchange reaction from building blocks **6a** and **b** is particularly useful to produce rotaxanes with different amide stoppers as shown with the preparation of compound **10**. However, reaction of **6a** and **b** with a relatively small amine reagent should promote the disassembly of the rotaxane structure and thus provide the corresponding components separately. As the mono-functionalization is by far more efficient and selective for rotaxane building block **1** when compared to model compound **2**, rotaxanes such as **6a** and **b** appear to be attractive building blocks for the efficient preparation of dissymmetrical axle products. In this case, the pillar[5]arene moiety plays the role of a *recyclable protecting group* allowing the successive introduction of two different terminal amide subunits onto axle **2**. In this respect, amine **11** was selected as the nucleophile (Scheme 4). Compounds **12a** and **b** were prepared by following two distinct synthetic routes,



Scheme 4. Preparation of dissymmetrical axles **12a** and **b** by following two different synthetic routes, and synthesis of rotaxane **15** with an elongated axle. i) THF, RT (from **4a**: **12a**: 95%; from **4b**: **12b**: 91%); ii) **11**, THF, RT (from **6a**: **12a**: 93% and **8**: 92%; from **6b**: **12b**: 92% and **8**: 97%); iii) **6a**, THF, RT (**14**: 69% and **8**: 99%); iv) **6b**, THF, RT (98%).

the first one is using rotaxane intermediates whereas the second one is based on the stepwise functionalization of the axle. As already discussed, the mono-functionalization of **2** with amines **3 a** and **b** was poorly selective thus leading to **4 a** and **b** in moderate yield. Moreover, the purification of both **4 a** and **b** by column chromatography on SiO₂ was particularly difficult owing to the formation of significant amounts of bis-amide byproducts (**5 a** and **b**) close in polarity. Treatment of **4 a** and **b** with amine **11** afforded dissymmetrical axle **12 a** and **b** in good yields. These compounds were then prepared by using the rotaxane strategy. In contrast to the first synthesis, high yields were obtained for the first step leading to rotaxane building blocks **6 a** and **b**. The selective mono-functionalization of **1** is a clear advantage as it prevents difficult purifications and is thus by far more convenient. Reaction of **6 a** and **b** with amine **11** finally provided **12 a** and **b** in good yields together with pillar[5]arene **8** that escaped the axle upon reaction with **11** because the methoxyethyl group is too small to act as a stopper to preserve the rotaxane structure. The two products were conveniently separated by column chromatography. Importantly, over 90% of pillar[5]arene **8** was recovered in both cases. Recycling of the pillar[5]arene protecting group is therefore effective. Not only the synthetic route using rotaxane building blocks was more convenient from a practical point of view due to easier purifications, the overall yields for the preparation of **12 a–b** over the two steps were also much higher (91 vs. 63% for **12 a** and 89 vs. 55% for **12 b**).

This strategy was then applied to prepare a [2]rotaxane with an elongated axle (Scheme 4). Reaction of **6 a** with a large excess of diamine **13** (5 equiv.) in THF gave **14** as well as pillar[5]arene **8**. Compound **14** was then isolated in 69% yield. The pillar[5]arene protecting group was also recovered in 99% yield. It can be noted that the preparation of amine **14** was also attempted by direct treatment of **4 a** with an excess of **13** (5 equiv.). In this particular case, the purification of **14** was very difficult owing to the formation of large amounts of diacetylated byproducts and the isolated yield was lower (47%). Finally, treatment of amine **14** with building block **6 b** in THF at room temperature gave **15** in 98% yield. With its very long axle component, [2]rotaxane **15** is an extended analogue of **10**.

Conformation analysis

With rotaxanes **10** and **15** in hand, the shuttling processes of the pillar[5]arene macrocycle along their axle were then investigated in detail.^[16] In the solid state, the pillar[5]arene subunit of rotaxane **10** is located close to the electron-rich dimethoxyphenyl stopper. As already mentioned for **6 a** and **b**, this peculiar conformation generates the most favorable intermolecular interactions within the crystal lattice of **10** but is not necessarily correlated with the conformational preferences of rotaxane **10** in solution. Obviously, one may expect random gliding motions of the pillar[5]arene moiety all along its decyl axis. However, some specific discrete positions maybe favored owing to the nature of the stopper or through the establishment of H-bonding interactions between one of the NH groups of the axle and an O atom of the pillar[5]arene component. This prompted us to analyze in details the ¹H NMR spectra recorded for rotaxane **10** at different temperatures and in different solvents (Figure 5 and Figure S2b in the Supporting Information). In addition, the NMR data of rotaxane **10** were systematically compared to those of model compounds (**5 a–b** and **7 a–b**). Furthermore, model axle **16** was also synthesized for comparison purposes (Scheme 5).

The chemical shifts observed for the methylene moieties of the $-(CH_2)_{10}-$ chain in the ¹H NMR of **10**, **5 a–b**, **7 a–b** and **16** are gathered in Table 3. In all the cases, 2D NMR COSY and ROESY spectra were analyzed for an unambiguous assignment of all the signals. For rotaxanes **10** and **7 a–b**, the resonances arising from their axle moieties are clearly distinguished. When compared to **5 a–b** and **16**, the important shielding observed for the protons of the methylene groups of the $-(CH_2)_{10}-$ linker provides a diagnostic signature for the interlocked structure of **10** and **7 a–b** (Table 3, Figure S1). For both symmetrical rotaxanes, all the signals of the CH₂ units of the decyl chain are affected by the ring current effect of the aromatic ring of their pillar[5]arene component. The shielding is however more important for H(3,4) in the case of **7 a** and for H(7,8) in the case of **7 b** showing that these particular methylene groups have a higher probability of presence in the cavity of the macrocycle. In other words, the pillar[5]arene moieties are preferentially located on the periphery of the axle. However, gliding motions of the pillar[5]arene from one end to the other of the axle are faster than the NMR timescale under these conditions as the two stoppers appear as equivalent. It can be also noted that the

Table 3. Chemical shifts (δ in ppm) of the methylene units of the $-(CH_2)_{10}-$ chain in the ¹H NMR spectra recorded at 25 °C in CD₂Cl₂ for compounds **10**, **7 a–b**, **5 a–b** and **16**. For clarity, the proton numbering used for **10** has been kept to assign the corresponding protons in symmetrical rotaxanes **7 a–b** and in axles **5 a–b** and **16** (see Figures 5 and S1).

Compound	H(1)	H(2)	H(3)	H(4)	H(5)	H(6)	H(7)	H(8)	H(9)	H(10)
10	1.81	0.93	0.27	0.17	0.17	−0.03	−0.83	−1.17	−0.13	1.23
7 a	1.56	0.51	−0.46	−0.46	0.00					
7 b						0.19	−0.29	−0.49	0.37	1.51
16	2.23	1.64	1.28	1.28	1.28	1.28	1.28	1.28	1.64	2.18
5 a	2.23	1.62	1.29	1.29	1.29					
5 b						1.27	1.27	1.27	1.61	2.16

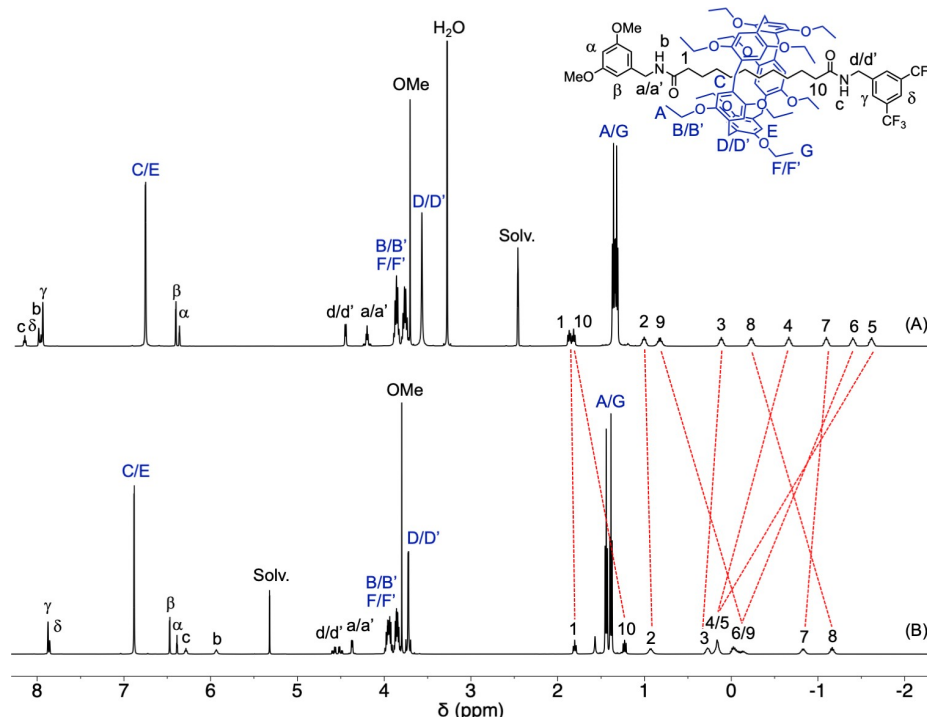


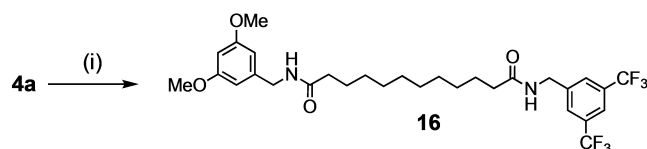
Figure 5. ^1H NMR spectra (400 MHz) recorded for rotaxane **10** in A) $[\text{D}_6]$ DMSO and B) CD_2Cl_2 at 298 K. For clarity, the proton numbering used for **10** has been kept to assign the corresponding protons in symmetrical rotaxanes **7a** and **b**.

nature of the stopper has an influence on the preferential positions of the macrocycle.

The multiplicity of the two diastereotopic benzylic methylene groups are effectively different in **7a** and **7b**. A doublet of AB is observed for H(d/d') in **7b** showing an effective transfer of the chiral information from the pillar[5]arene to this methylene group in agreement with a high probability of presence of the macrocycle close to the periphery. In contrast, the chiral information transfer is not effective in the case of **7a**. Effectively, H(a/a') appears as a doublet in **7a** at room temperature. This observation suggests that the pillar[5]arene has a lower probability of presence in the peripheral positions within **7a** when compared to **7b**. It seems therefore that weak through space interactions between the electron-rich pillar[5]arene moiety and the stopper may also play a role in the distribution of all the possible conformers in rotaxanes **7a** and **b**. These very weak intramolecular polar interactions are obviously more attractive in the case of the electron-deficient bis(trifluoromethyl)phenyl stopper (**7b**) when compared to the electron-rich dimethoxyphenyl stopper (**7a**). In the case of unsymmetrically substituted rotaxane **10** the most important shielding is observed for the signals arising from the methylene

groups H(7,8) of the $-(\text{CH}_2)_{10}-$ axle. Therefore, the macrocycle is preferentially located close to the most electro-deficient bis-(trifluoromethyl)phenyl stopper. This view is also fully supported by the comparison of the chemical shifts of the methylene groups in **10** with those in **7a–b**. Effectively, when compared to **7b**, the resonances of H(7,8) are significantly upfield shifted in **10**. At the same time, the resonances of H(3,4) are downfield shifted when going from **7a** to **10**. Moreover, a doublet of AB is observed for H(d/d') showing an effective transfer of the chiral information from the pillar[5]arene to this methylene group. In contrast, the chiral information transfer is not effective in the case of H(a/a'). This is also in full agreement for a higher population of conformers in which the macrocycle is close to the electron-deficient stopper.

To further understand the dynamic conformational equilibrium of **10** and **7a–b**, ^1H NMR spectra were also recorded at different temperatures (Figure S2a and b). If there are effectively energetically favored conformations, their population should be increased by lowering the temperature. In all the cases, limited chemical shift changes are observed for the signals of the decyl chain of the axle but the upfield shift observed by lowering the temperature for the resonances of H(7,8) in **10** and **7b** is consistent with a slight preference for conformations in which these particular methylene groups are within the cavity of the pillar[5]arene. Similar upfield shifts are also observed for the resonances of H(3,4) in both **10** and **7a**. Therefore, peripheral positions of the macrocycle are also favored for the electron-rich stopper. Clearly, conformations in which the pillar[5]arene subunit are located close to the stoppers are slightly energetically favored whatever the nature of the stopper. The stabiliza-



Scheme 5. Preparation of model compound **16**. i) **3b**, THF, RT (94%).

tion is however more pronounced when the stopper is electron-deficient as shown by the difference in chemical shift observed for H(3,4) and H(7,8) in the case of rotaxane **10**. On the other hand, in all the cases, transfer of the chiral information from the pillar[5]arene to the benzylic methylene groups H(a/a') and H(d/d') is more and more effective when lowering the temperature. This is also in complete agreement with a higher probability of presence of the chiral macrocycle on the peripheral positions close to these diastereotopic CH₂ moieties when lowering the temperature. The energy barrier to switch from one peripheral position to the other is however low as the dynamic exchange is still faster than the NMR timescale at 208 K for all the rotaxanes. Overall, detailed analysis of the NMR data recorded in CD₂Cl₂ for compounds **10** and **7a–b** revealed fast dynamic gliding motions of the macrocycle along the decyl chains of the axle. Conformations in which the pillar[5]arene is close to the stopper are slightly stabilized by either polar interactions and/or the occurrence of intramolecular H-bonding interactions. In the particular case of **10**, additional weak through space donor-acceptor attractive interactions between the bis(trifluoromethyl)phenyl moiety and the pillar[5]arene contribute to further stabilize conformations in which the macrocycle is close to its electron-deficient stopper. The influence of the different amide stoppers on the conformational equilibria observed for rotaxanes **10** and **7a–b** was also in agreement with the differences observed for the *K_A* values of the host-guest complexes obtained from model compounds **9a–b** and pillar[5]arene **8** (Figure 5). The *meta*-substituents of the terminal benzylic groups have effectively an effect on the *K_A* values, the formation of the host-guest complex being more favorable for the guest with the electron-deficient bis(trifluoromethyl)benzyl substituent. This is fully consistent with the influence of the different stoppers on the conformation observed in the case of rotaxane **10**. The difference in Gibbs free energy ($\Delta\Delta G^\circ$) between **9a** and **9b** is 2.5 kJ mol⁻¹ under the experimental conditions used for the binding studies (CDCl₃, 298 K). This small energy difference is sufficient to significantly influence the Maxwell-Boltzmann distribution of the different possible conformers of **10** and explains well why the peripheral position of the pillar[5]arene close to the bis(trifluoromethyl)benzyl stopper is favored.

In order to evaluate the role of hypothetical H-bonding interactions between the NH groups of the axle subunit and the O atoms of the pillar[5]arene moiety in rotaxanes **10** and **7a–b**, a competitive H-bonding donor/acceptor was added to CD₂Cl₂ solutions of **10** and **7a–b**. The observed changes upon addition of methanol to CD₂Cl₂ solutions of **10** and **7a–b** are shown in Figure S3. Only very minor changes in chemical shifts were detected for the resonances of the methylene moieties of the decyl chains. Therefore, the average position of the macrocycle on the axle of **10** and **7a–b** is not affected by the presence of an excess of methanol thus showing that H-bonding plays only a very minor role if any in the preferential peripheral positions of the macrocyclic component on the axle of the rotaxane. The conformation of **10** and **7a–b** is therefore mainly governed by weak dipole-dipole interactions in a non-polar organic solvent such as methylene chloride. This view is also consistent with

the conformational preferences observed for rotaxanes **6a–e**. For all these compounds, the macrocyclic component is preferentially located close to its pentafluorophenyl ester stopper despite possible additional intercomponent H-bonding interactions between the NH of the other stopper with an O atom of the pillar[5]arene subunit (see below).

To further understand the conformational preferences of rotaxanes of **10** and **7a–b**, ¹H NMR spectra were also recorded in polar organic solvents, namely [D₆]DMSO and/or [D₇]DMF. Under these conditions, polar interactions are expected to be disfavored while solvophobic effects are expected to be stronger.^[17] The ¹H NMR spectra recorded for **10** and **7a–b** in different solvents are shown in Figures 5 and S4. In all the cases, dramatic chemical shift changes were observed for the resonances of the methylene groups of the decyl chain when going from a nonpolar to a polar solvent. The position of the pillar[5]arene moiety on its axle moiety is actually highly sensitive to the solvent polarity. Analysis of the relative chemical shifts of the methylene groups in **10** and **7a–b** revealed that the pillar[5]arene moiety is preferentially located in the middle of the decyl chains in polar media. The Maxwell-Boltzmann distribution of all the possible conformers is therefore highly sensitive to the solvent polarity. In nonpolar solvents (CH₂Cl₂ or CHCl₃), intramolecular dipole-dipole interactions play a major role. As a result, conformations in which the macrocycle is close to its stoppers are favored. When the two stoppers are different as in the case of **10**, the peripheral position close to the most electron-deficient stopper is more populated owing to favorable trough-space donor-acceptor interactions. In contrast, such polar interactions are disfavored in polar solvents (DMSO or DMF). Solvophobic effects are actually dominating the conformational preferences of **10** and **7a–b**. Obviously, the terminal amide functions of **10** and **7a–b** are well solvated by DMF or DMSO while repulsive interactions between the decyl chain and the polar solvent molecules are expected. As a result, the macrocycle is preferentially located in the middle of the axle subunit to limit unfavorable interactions between the decyl chain and the solvent.

Conformational analysis of rotaxane **15** with a longer axle was also carried out based on NMR studies. The ¹H NMR of **15** recorded in CDCl₃ at room temperature is depicted in Figure 6. Considering the shielding effect of the pillar[5]arene moiety on the resonances of the methylene groups located within its cavity, it appears clear that the macrocycle is located over the two decyl subunits of the axle (stations 1 and 3). The dynamic exchange by gliding motions must be however close to the NMR timescale under these conditions as some signals of the decyl chain are broadened. In contrast, the chemical shifts of the CH₂ groups of the tri(ethylene glycol) spacer are observed at regular chemical shifts thus showing that the macrocycle is on average not preferentially located on the tri(ethylene glycol) station of its axle unit. To fully confirm the fast gliding motions of the macrocycle all over its molecular string, variable temperature NMR studies were carried out. The ¹H NMR spectra of **15** recorded at various temperature are shown in Figures S5 and S6. By increasing the temperature, a perfectly reversible narrowing is observed for the signals of the methylene groups

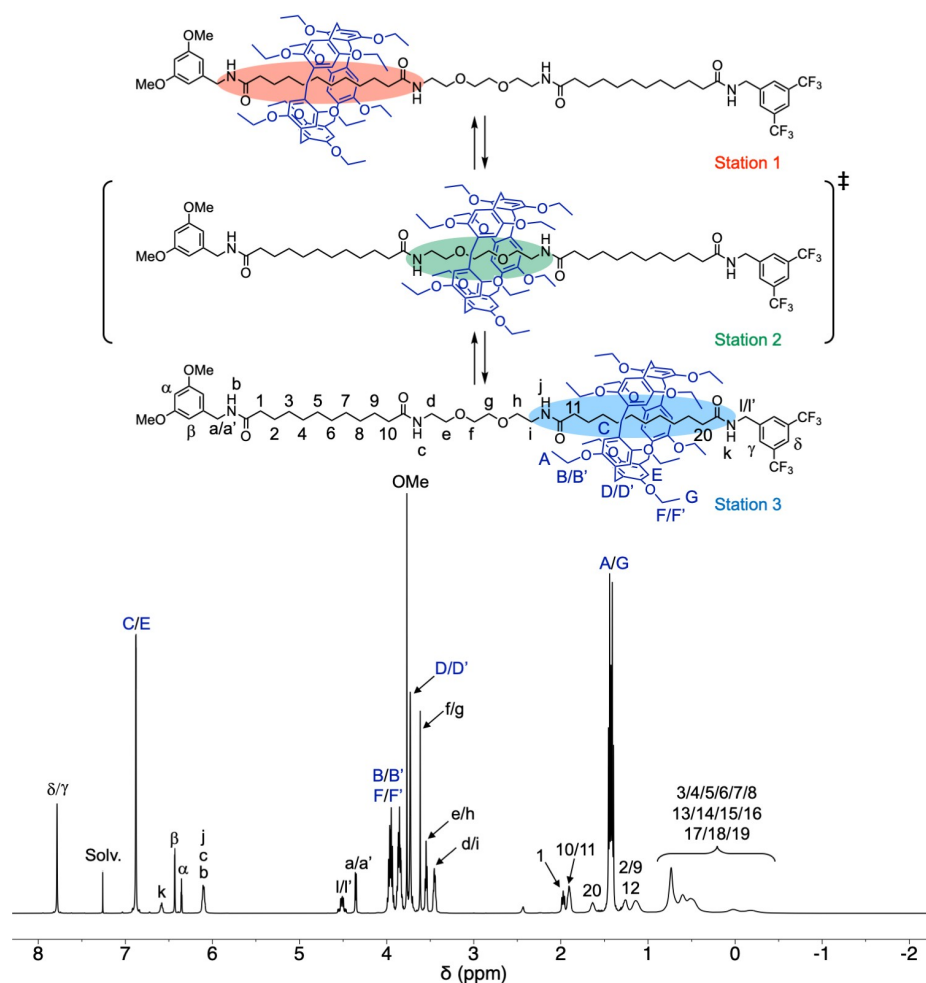


Figure 6. ^1H NMR spectrum (500 MHz) of compound **15** recorded in CDCl_3 at 298 K and conformational equilibrium deduced from the variable temperature studies.

of the decyl moieties. At high temperature, the dynamic exchange between the two possible conformers in which the pillar[5]arene is located over one or the other decyl station is faster than the NMR timescale. In contrast, at low temperature, the dynamic exchange becomes slower than the NMR timescale and the ^1H NMR spectrum recorded at 208 K in CD_2Cl_2 corresponds to the superposition of the spectra of two conformers differing by the position of the pillar[5]arene over its axle (Figure S6). The macrocycle is either located over one or the other decyl station. A detailed analysis of the spectrum recorded at this temperature revealed that the relative proportion of the two conformers is similar. Based on the integration, a 56:44 ratio is deduced, the major conformer being the one in which the decyl station bearing the bis-(trifluoromethyl)benzyl stopper (station 3) is occupied. Based on a Boltzmann population analysis at 208 K, this corresponds to an average difference of energy lower than 1 kJ mol^{-1} between the two conformations. The attractive effect of the electron-deficient stopper is very weak and clearly not sufficient to obtain a perfect conformational control in rotaxane **15**. Moreover, dynamic gliding motions of the macrocycle over the long axle of **15** generate a large number of possible conformations

relatively close in energy. Considering the Maxwell–Boltzmann population of all these discrete conformers in dynamic exchange, the multiplication of possible positions for the macrocycle limits also the occupancy of the energetically favored one as its additional stabilization is very weak. The free energy of activation ΔG^\ddagger for the dynamic exchange was obtained by analyzing the coalescence of several signals. The ΔG^\ddagger value thus deduced is $47 \pm 1 \text{ kJ mol}^{-1}$. Overall, the variable temperature NMR studies of rotaxane **15** revealed that pillar[5]arene is preferentially located over its two decyl stations. Due to the presence of the bis(trifluoromethyl)benzyl stopper, station 3 is slightly favored but the attractive effect between the electron-rich pillar[5]arene and the electron-deficient stopper is extremely weak. In contrast, station 2 is not significantly populated by the macrocycle and can be considered as the transition state for the dynamic exchange allowing the macrocycle to shuttle back and forth between the two different decyl stations. At high temperature, dynamic exchange between the two degenerate states is faster than the NMR timescale. In contrast, the two conformers are clearly distinguished at low temperature.

Conclusions

In this paper, we have reported detailed investigations into the mono-functionalization of rotaxane building block **1** bearing two equivalent pentafluorophenyl ester stoppers. Upon a first stopper exchange, the pillar[5]arene moiety of the mono-acylated product is preferentially located close to its reactive pentafluorophenyl ester stopper. As a result, it is more difficult for the nucleophilic reagents to access the reactive carbonyl group, thus allowing the efficient preparation of mono-amide rotaxanes from **1**. The synthetic utility of the resulting building blocks bearing only one activated stopper has been demonstrated with the efficient preparation of dissymmetrical rotaxanes **10** and **15**. We have also shown that the pillar[5]arene can act as a protecting group for the synthesis of dissymmetrical axles that are particularly difficult to prepare under statistical conditions. Finally, conformation analysis of rotaxanes **10** and **15** revealed a fast gliding motion of the pillar[5]arene component over its axle subunit. Conformers in which the pillar[5]arene moiety is located close to its most electron-deficient stopper are slightly energetically favored in solution in the case of rotaxane **10** with a relatively short axle unit. Similar effects are, however, limited in the case of rotaxane **15** with an elongated axle moiety. Weak energy differences resulting from through-space donor–acceptor interactions and intramolecular dipole–dipole interactions are not sufficient to control the position of the macrocycle on a very long axle unit. In the case of **15**, a much higher number of conformers is possible. As they are all close in energy, their Maxwell–Boltzmann distribution is not favorable to significantly populating a higher proportion of the conformer in which the macrocycle is close to its electron-deficient stopper.

Experimental Section

Synthesis. The preparation and characterization of all the new compounds are described in the Supporting Information. Compounds **1**,^[12] **2**^[12] and **8**^[18] were prepared according to reported procedures. Representative experimental procedures:

General procedure for the preparation of [2]rotaxanes 6a–e. A mixture of **1** (2.0 equiv.) and the appropriate primary amine reagent (**3a–e**, 1.0 equiv.) in anhydrous THF (1 mL/110 mg of **1**) was stirred at 0 °C for 3 h. The resulting mixture was filtered through a short plug (SiO₂, CH₂Cl₂), concentrated and purified by column chromatography on SiO₂ followed by gel permeation chromatography (Biobeads SX-1, CH₂Cl₂).

General procedures for the preparation of [2]rotaxanes 6f–g. A mixture of **1** (2.0 equiv.) and the appropriate secondary amine reagent (**3f–g**, 1.0 equiv.) in anhydrous THF (1 mL/110 mg of **1**) was stirred at RT for 6 days (**6f**) or 4 days (**6g**). The resulting mixture was filtered through a short plug (SiO₂, CH₂Cl₂), concentrated and purified by column chromatography on SiO₂ followed by gel permeation chromatography (Biobeads SX-1, CH₂Cl₂).

Preparation of compound 10. A mixture of **6b** (0.439 g, 0.29 mmol) and **3a** (0.059 g, 0.35 mmol) in anhydrous THF (3 mL) was stirred at RT overnight. The resulting mixture was filtered through a short plug (SiO₂, CH₂Cl₂ containing 2% MeOH) and concentrated. Column chromatography (SiO₂, CH₂Cl₂ containing 2% MeOH) followed by

gel permeation chromatography (Biobeads SX-1, CH₂Cl₂) afforded **10** (0.419 g, 98%).

Preparation of compound 12a. A solution of **6a** (0.172 g, 0.12 mmol) and **11** (0.010 g, 0.13 mmol) in anhydrous THF (1.5 mL) was stirred at RT. After 3 h, the reaction mixture was concentrated. Column chromatography (SiO₂, cyclohexane/CH₂Cl₂ (1:1) to CH₂Cl₂ containing 3% MeOH) gave compound **8** (0.098 g, 92%) and compound **12a** (0.049 g, 93%).

X-ray crystal structures: the crystallographic data and the refinement parameters are reported in the Supporting Information for all the compounds. Deposition Numbers 2302604 (for **6a**), 2302607 (for **6b**) and 2302603 (for **10**) contain the supplementary crystallographic data for this paper. These data are provided free of charge by the joint Cambridge Crystallographic Data Centre and Fachinformationszentrum Karlsruhe Access Structures service.

Supporting Information

The authors have cited additional references within the Supporting Information.^[19,20]

Acknowledgements

Financial support from the ANR (projects FastGiant ANR-17-CE07-0012-01 and Pillar ANR-19-CE06-0032), the *Fondation Jean-Marie Lehn*, the LabEx “*Chimie des Systèmes Complexes*”, and the Tunisian Ministry of Higher Education and Scientific Research and Technology is gratefully acknowledged. We thank C. Bailly and N. Gruber for the X-ray crystal structure resolution. We also thank Dr. M. Holler for helpful discussions.

Conflict of Interests

The authors declare no conflict of interest.

Data Availability Statement

The data that support the findings of this study are available in the supplementary material of this article.

Keywords: molecular shuttles · pillararenes · protecting groups · rotaxanes · stopper exchange

- [1] a) J.-P. Sauvage, C. Dietrich-Buchecker, *Molecular Catenanes, Rotaxanes and Knots: A Journey through the World of Molecular Topology*, Wiley, 2008; b) C. J. Brun, J. F. Stoddart, *The Nature of the Mechanical Bond: From Molecules to Machines*, Wiley, 2016.
- [2] R. Brückner, *Eur. J. Org. Chem.* 2019, 3289–3319.
- [3] a) R. A. Bissell, E. Córdova, A. E. Kaifer, J. F. Stoddart, *Nature* 1994, 369, 133–137; b) A. Livoreil, C. O. Dietrich-Buchecker, J.-P. Sauvage, *J. Am. Chem. Soc.* 1994, 116, 9399–9400.
- [4] a) J.-P. Sauvage, *Angew. Chem. Int. Ed.* 2017, 56, 11080–11093; *Angew. Chem.* 2017, 129, 11228–11242; b) J. F. Stoddart, *Angew. Chem. Int. Ed.* 2017, 56, 11228–11242; *Angew. Chem.* 2017, 129, 11244–11277.
- [5] a) V. Balzani, A. Credi, M. Venturi, *Molecular Devices and Machines: A Journey into the Nano World*, Wiley-VCH, Weinheim, 2003; b) E. R. Kay,

- D. A. Leigh, *Angew. Chem. Int. Ed.* **2015**, *54*, 10080–10088; *Angew. Chem.* **2015**, *127*, 10218–10226; c) S. Erbas-Cakmak, D. A. Leigh, C. T. McTernan, A. L. Nussbaumer, *Chem. Rev.* **2015**, *115*, 10081–10206; d) D. A. Leigh, *Angew. Chem. Int. Ed.* **2016**, *55*, 14506–14508; *Angew. Chem.* **2016**, *128*, 14722–14724; e) S.-J. Rao, Q. Zhang, J. Mei, X.-H. Ye, C. Gao, Q.-C. Wang, D.-H. Qu, H. Tian, *Chem. Sci.* **2017**, *8*, 6777–6783; f) S.-J. Rao, K. Nakazono, X. Liang, K. Nakajima, T. Takata, *Chem. Commun.* **2019**, *55*, 5231–5234; g) Q. Zhang, S.-R. Rao, T. Xie, X. Li, T.-Y. Xu, D.-W/ Li, D.-H. Qu, Y.-T. Long, H. Tian, *Chem* **2018**, *4*, 2670–2684; h) S. Corra, M. Curcio, M. Baroncini, S. Silvi, A. Credi, *Adv. Mater.* **2020**, *32*, 1906064; i) M. Baroncini, S. Silvi, A. Credi, *Chem. Rev.* **2020**, *120*, 200–268; j) C.-S. Kwan, K. C.-F. Leung, *Mater. Chem. Front.* **2020**, *4*, 2825–2844; k) H.-Y. Zhou, Y. Han, C.-F. Chen, *Mater. Chem. Front.* **2020**, *4*, 12–28.
- [6] P. Waelès, M. Gauthier, F. Coutrot, *Angew. Chem. Int. Ed.* **2021**, *60*, 16778–16799.
- [7] a) S. Anderson, T. D. W. Claridge, H. L. Anderson, *Angew. Chem. Int. Ed.* **1997**, *36*, 1310–1313; *Angew. Chem.* **1997**, *109*, 1367–1370; b) J. E. H. Buston, J. R. Young, H. L. Anderson, *Chem. Commun.* **2000**, 905–906; c) F. Cacialli, J. S. Wilson, J. J. Michels, C. Daniel, C. Silva, R. H. Friend, N. Severin, P. Samori, J. P. Rabe, M. J. O'Connell, P. N. Taylor, H. L. Anderson, *Nat. Mater.* **2002**, *1*, 160–164; d) M. J. Frampton, H. L. Anderson, *Angew. Chem. Int. Ed.* **2007**, *46*, 1028–1064; *Angew. Chem.* **2007**, *119*, 1046–1083.
- [8] Similar protecting effects have been also reported for squaraine-containing rotaxanes, see: a) E. Arunkumar, C. C. Forbes, B. C. Noll, B. D. Smith, *J. Am. Chem. Soc.* **2005**, *127*, 3288–3289; b) J. Gassensmith, J. M. Baumes, B. D. Smith, *Chem. Commun.* **2009**, 6329–6338.
- [9] a) L. D. Movsisyan, D. V. Kondratuk, M. Franz, A. L. Thompson, R. R. Tykwinski, H. L. Anderson, *Org. Lett.* **2012**, *14*, 3424–3426; b) N. Weisbach, Z. Baranova, S. Gauthier, J. H. Reibenspies, J. A. Gladysz, *Chem. Commun.* **2012**, *48*, 7562–7564; c) H. Sahnoune, Z. Baranova, N. Bhuvanesh, J. A. Gladysz, J.-F. Halet, *Organometallics* **2013**, *32*, 6360–6367; d) L. D. Movsisyan, M. D. Peeks, G. M. Greetham, M. Towrie, A. L. Thompson, A. W. Parker, H. L. Anderson, *J. Am. Chem. Soc.* **2014**, *136*, 17996–18008; e) M. Franz, J. A. Januszewski, D. Wendinger, C. Neiss, L. D. Movsisyan, F. Hampel, H. L. Anderson, A. Gçrling, R. R. Tykwinski, *Angew. Chem. Int. Ed.* **2015**, *54*, 6645–6649; *Angew. Chem.* **2015**, *127*, 6746–6750; f) L. D. Movsisyan, M. Franz, F. Hampel, A. L. Thompson, R. R. Tykwinski, H. L. Anderson, *J. Am. Chem. Soc.* **2016**, *138*, 1366–1376; g) D. R. Kohn, L. D. Movsisyan, A. L. Thompson, H. L. Anderson, *Org. Lett.* **2017**, *19*, 348–351; h) D. C. Milan, M. Kremppe, A. K. Ismael, L. D. Movsisyan, M. Franz, I. Grace, R. J. Brooke, W. Schwarzacher, S. J. Higgins, H. L. Anderson, C. J. Lambert, R. R. Tykwinski, R. J. Nichols, *Nanoscale* **2017**, *9*, 355–361; i) M. Franz, J. A. Januszewski, F. Hampel, R. R. Tykwinski, *Eur. J. Org. Chem.* **2019**, *2019*, 3503–3512.
- [10] a) A. H. Parham, B. Windisch, F. Vögtle, *Eur. J. Org. Chem.* **1999**, *1999*, 1233–1238; b) D. A. Leigh, E. M. Perez, *Chem. Commun.* **2004**, 2262–2263; c) A. Mateo-Alonso, P. Brough, M. Prato, *Chem. Commun.* **2007**, 1412–1414; d) F. Scarel, G. Valenti, S. Gaikwad, M. Marcaccio, F. Paolucci, A. Mateo-Alonso, *Chem. Eur. J.* **2012**, *18*, 14063–14068; e) D. M. D'Souza, D. A. Leigh, L. Mottier, K. M. Mullen, F. Paolucci, S. J. Teat, S. Zhang, *J. Am. Chem. Soc.* **2010**, *132*, 9465–9470; f) N. Kihara, Y. Tachibana, H. Kawasaki, T. Takata, *Chem. Lett.* **2000**, *29*, 506–507; g) J. Winn, A. Pinczewska, S. Goldup, *J. Am. Chem. Soc.* **2013**, *135*, 13318–13321.
- [11] a) I. Nierengarten, E. Meichsner, M. Holler, P. M. Pieper, R. Deschenaux, B. Delavaux-Nicot, J.-F. Nierengarten, *Chem. Eur. J.* **2018**, *24*, 169–177; b) I. Nierengarten, J.-F. Nierengarten, *ChemistryOpen* **2020**, *9*, 393–400.
- [12] M. Rémy, I. Nierengarten, B. Park, M. Holler, U. Hahn, J.-F. Nierengarten, *Chem. Eur. J.* **2021**, *27*, 8492–8499.
- [13] The post-modification of pre-constructed [2]rotaxanes by stopper exchange reactions has been rarely used and only a few examples have been reported so far, see: a) S. J. Rowan, J. F. Stoddart, *J. Am. Chem. Soc.* **2000**, *122*, 164–165; b) S. J. Rowan, S. J. Cantrill, J. F. Stoddart, A. J. P. White, D. J. Williams, *Org. Lett.* **2000**, *2*, 759–762; c) R. J. Bordoli, S. M. Goldup, *J. Am. Chem. Soc.* **2014**, *136*, 4817–4820; d) D. W. Zehnder II, D. B. Smithrud, *Org. Lett.* **2001**, *3*, 2485–2487; e) N. Kihara, S. Motoda, T. Yokozawa, T. Takata, *Org. Lett.* **2005**, *7*, 1199–1202; f) J. S. Hannam, S. M. Lacy, D. A. Leigh, C. G. Saiz, A. M. Z. Slawin, S. G. Stithell, *Angew. Chem. Int. Ed.* **2004**, *43*, 3260–3264; g) S. C. Rajappan, D. R. McCarthy, J. P. Campbell, J. B. Ferrel, M. Sharafi, O. Ambrozaite, J. Li, S. T. Schneebeli, *Angew. Chem. Int. Ed.* **2020**, *59*, 16668–16674.
- [14] Dissymmetrical pillar[5]arene-containing [2]rotaxanes prepared by the introduction of a stopper to a dissymmetrical axle have been reported, see: a) M. Steffenhagen, A. Latas, T. M. N. Trinh, I. Nierengarten, I. T. Lucas, S. Joiret, J. Landoulsi, B. Delavaux-Nicot, J.-F. Nierengarten, E. Maisonhaute, *Chem. Eur. J.* **2018**, *24*, 1701–1708; b) B. Delavaux-Nicot, H. Ben Aziza, I. Nierengarten, T. M. N. Trinh, E. Meichsner, M. Chessé, M. Holler, P. R. Abidi, E. Maisonhaute, J.-F. Nierengarten, *Chem. Eur. J.* **2018**, *24*, 133–140; c) G. Boitel-Aullen, L. Fillaud, F. Huet, I. Nierengarten, B. Delavaux-Nicot, J.-F. Nierengarten, E. Maisonhaute, *ChemElectroChem* **2021**, *8*, 3506–3511.
- [15] a) L. Gao, C. Han, B. Zheng, S. Dong, F. Huang, *Chem. Commun.* **2013**, *49*, 472–474; b) T. M. N. Trinh, I. Nierengarten, M. Holler, J.-L. Gallani, J.-F. Nierengarten, *Chem. Eur. J.* **2015**, *21*, 8019–8022; c) M. Holler, T. Stoerkler, A. Louis, F. Fisher, J.-F. Nierengarten, *Eur. J. Org. Chem.* **2019**, 3401–3405.
- [16] For other example of conformational analysis of pillar[n]arene-based rotaxanes, see: a) T. Ogoshi, D. Yamafuji, T. Aoki, T.-A. Yamagishi, *Chem. Commun.* **2012**, *48*, 6848–6844; b) T. Ogoshi, D. Yamafuji, T. Aoki, K. Kitajima, T.-A. Yamagishi, Y. Hayashi, S. Kawachi, *Chem. Eur. J.* **2012**, *18*, 7493–7500; c) S. Dong, C. Han, B. Zheng, M. Zhang, F. Huang, *Tetrahedron Lett.* **2012**, *53*, 3668–3671; d) S. Dong, J. Yuan, F. Huang, *Chem. Sci.* **2014**, *5*, 247–252; e) Y. Liu, C. Chipot, X. Shao, W. Cai, *J. Phys. Chem. C* **2016**, *120*, 6287–6293; f) S. Wang, X. Shao, W. Cai, *J. Phys. Chem. C* **2017**, *121*, 25547–25553; g) P. Wei, X. Yan, J. Li, Y. Ma, Y. Yao, F. Huang, *Tetrahedron* **2012**, *68*, 9179–9185.
- [17] J. L. Cook, C. A. Hunter, C. M. R. Low, A. Perez-Velasco, J. G. Vinter, *Angew. Chem. Int. Ed.* **2007**, *46*, 3706–3709; *Angew. Chem.* **2007**, *119*, 3780–3783.
- [18] a) T. Ogoshi, K. Kitajima, T. Aoki, S. Fujinami, T.-A. Yamagishi, Y. Nakamoto, *J. Org. Chem.* **2010**, *75*, 3268–3273; b) M. Holler, N. Allenbach, J. Sonet, J.-F. Nierengarten, *Chem. Commun.* **2012**, *48*, 2576–2578.
- [19] D. D. Günbas, A. M. Brouwer, *J. Org. Chem.* **2012**, *77*, 5724–5735.
- [20] a) C. Frassinetti, S. Ghelli, P. Gans, A. Sabatini, M. S. Moruzzi, A. Vacca, *Anal. Biochem.* **1995**, *231*, 374–382; b) C. Frassinetti, L. Alderighi, P. Gans, A. Sabatini, A. Vacca, S. Ghelli, *Anal. Bioanal. Chem.* **2003**, *376*, 1041–1052.

Manuscript received: October 24, 2023

Accepted manuscript online: November 20, 2023

Version of record online: December 21, 2023